Astron. Astrophys. 318, 783–790 (1997)

ASTRONOMY
AND
ASTROPHYSICS

The pre-main-sequence spectroscopic binary NTTS 162814-2427: models versus observations

J. Figueiredo⋆

Departamento de Matemática da Universidade do Minho, Campus de Gualtar, 4700 Braga, Portugal

Received 30 January 1996 / Accepted 22 May 1996

Abstract. Models of stars with masses between 0.5 and 1.5 $M_{\odot}$ evolving in the pre-main-sequence (PMS) have been computed using a multiple shooting point hydrodynamic code. The theoretical results are compared with the most recent observational data available for the double-lined PMS spectroscopic binary NTTS 162814-2427. A comparison with theoretical models computed with different input physics concerning the opacities, the equation of state (EOS) and the convection treatment of superadiabatic regions is also done. Our reference model agrees well with the dynamical mass ratio and the assumption of coeval formation of the binary components. Accordingly, assuming a K4 primary and a K5 secondary we estimate the mass of the primary and secondary to be 1.10 and 1.00 $M_{\odot}$, respectively, with an age of 3.7 million years.

Key words: binaries: spectroscopic – stars: pre-main-sequence – stars: evolution – stars: fundamental parameters

1. Introduction

The double-lined PMS spectroscopic binaries are extremely useful tools to test the relative mass and age calibrations of theoretical evolutionary models. In fact, if theoretical masses can be determined for each component of such binaries, then theoretical mass ratios can be obtained and compared with the accurate dynamical mass ratios provided by these binaries. Furthermore, the assumption of coeval formation of the binary components can be used to constrain the theoretical mass-age calibrations even more (e.g. Mathieu 1994). On the other hand, the dynamical results obtained from the observation of such binaries provide lower mass limits for each component. Although these mass limits are generally too small to constrain the theoretical models in a relevant way, in some cases, however, their values are large enough to provide useful constraints to stellar models. As we will show later, this is precisely the case for the PMS double-lined spectroscopic binary NTTS 162814-2427, making this binary particularly suitable for testing purposes (see also Mathieu et al. 1989, hereafter MWM).

In the present work we make use of the most recent observational data available for the binary NTTS 162814-2427 and the hypothesis of coeval formation of its components as a test to sequences of PMS stellar models computed with a new hydrodynamic evolutionary code. In order to estimate the uncertainties on the mass and age determinations we computed models with different physical inputs concerning the low- and high-temperature opacities, the EOS and the treatment of convection. The method used for the comparison between theoretical and observational results also allows to estimate the uncertainties on the mass-age determinations due to the uncertainties in the effective temperature and luminosity of each component.

2. Observational data

The first detection of the binary NTTS 162814-2427 was made by Montmerle et al. (1983) in the X-ray wavelength band using the Einstein satellite. The binary, situated among the naked T Tauri population of the Scorpius Ophiuchus star-forming region, was later observed by MWM who obtained the corresponding orbital solution. From that orbital solution MWM derived a period of 35.95 $\pm$ 0.02 days and an eccentricity of 0.48 $\pm$ 0.01. They also obtained an estimate for the dynamical mass ratio of 1.09 $\pm$ 0.07 as well as a lower limit for the primary mass of 1.02 $\pm$ 0.06 $M_{\odot}$ and for the secondary mass of 0.94 $\pm$ 0.05 $M_{\odot}$. Adopting a single extinction value for both components, $A_V = 1.5 \pm 0.5$, they estimated the primary luminosity to be 1.0 $L_{\odot}$ and suggested this binary is composed of a K7 primary and a late-K secondary.

A more sophisticated study of the NTTS 162814-2427 binary was made by Lee (1992) using high-dispersion optical spectroscopy, low-dispersion spectrophotometry and broadband photometry, to investigate the characteristics of its components. The study suggests this binary is composed of K4 and K5 stars, allowing thus four possible primary-secondary spectral type combinations. For each of these combinations Lee derived the primary and secondary luminosities from the observed flux ratios. This was done using two different values for the parameter characterising the extinction law, R_V [$\equiv A_V/E(B-V)$], namely 3.1 and 5.0. The first corresponds to the value typically found in the diffuse interstellar medium, while the second was

⋆ also Centro de Astrofísica da Universidade do Porto

Table 1. Observational data for the binary NTTS 162814-2427 (Lee 1992). Effective temperatures were derived using the Cohen & Kuhi (1979) spectral type-effective temperature scale. Luminosities correspond to $R_V = 5.0$. Estimated errors are $\Delta \log T_{\rm eff} = 0.01$ and $\Delta \log L/L_\odot = 0.07$ (details in Sect. 5)

	p - s		p - s		p - s		p - s	
Sp. Type	K4	K4	K4	K5	K5	K4	K5	K5
$\log T_{\rm eff}$	3.661	3.661	3.661	3.643	3.643	3.661	3.643	3.643
$\log L/L_\odot$	0.11	-0.06	0.08	-0.07	0.09	-0.11	0.05	-0.13

obtained by Lee fitting extinction curves to his photometric results. We note that values of $R_{\rm V}$ greater than four have also been reported by Cardelli (1988) for stars in the Ophiuchus molecular cloud. On the other hand, Bouvier & Appenzeller (1991) obtained $A_V = 1.9$ for the NTTS 162814-2427 binary. This value is in better agreement with the one derived by Lee using $R_V = 5.0$ (1.9 ± 0.1) rather than $R_V = 3.1$ (1.6 ± 0.1). Therefore we adopt $R_V = 5.0$ in this work. Table 1 summarises the observational data available for the binary NTTS 162814-2427 relevant for this study.

3. Theoretical models

The theoretical models were calculated with a multiple shooting point (Wilson 1981) one-dimensional hydrodynamic code developed by us at the Centro de Astrofísica da Universidade do Porto and the Astrophysical Institute of Vrije Universiteit Brussel. This code assumes a spherically symmetrical model with no rotation and no magnetic fields. In the following sections we summarise the more relevant inputs of the code (details in Figueiredo 1996).

3.1. Equation of state

The EOS is computed using the so-called "chemical picture", yielding the pressure and internal energy as a function of temperature, density and chemical composition. The Saha equation is iteratively solved for the following species: H, H^+, He, He^+ and He^{++}. The formation of H_2 is also taken into account for temperatures below 10 000 K using the dissociation equilibrium constant of Sauval & Tatum (1984). The contribution of H^- to the EOS is not included. However, neglecting H^- should not affect our results in a significant way since the important role played by this ion as an opacity source is already included in the opacity tables we have used (see further).

The EOS applies to a semi-degenerated gas and includes ion, electron and radiation contributions, as well as corrections accounting for the formation of electron-positron pairs and the Coulomb interactions between charged particles. Coulomb corrections to the pressure and energy, as well as to the (laboratory) ionisation potentials, are considered. They are calculated using the numerical results obtained by Broyles et al. (1963) and Shaviv & Kovetz (1972). In the high-temperature low-density regime one recovers the results of the Debye-Hückel model (see e.g. Cox & Giuli 1968; Graboske et al. 1969). Pressure ionisation occurs each time the effective ionisation potential becomes negative.

3.2. Nuclear network

The nuclear network includes the p-p chains and the CNO tricycle (Clayton 1968). The thermonuclear reaction rates are computed using the analytical fitting formulae given by Caughlan & Fowler (1988) except for the ^{17}O(p,γ)^{18}F and ^{17}O(p,α)^{14}N reaction rates which are taken from Landré et al. (1990). Screening factors accounting for weak, intermediate and strong screening effects are computed according to DeWitt et al. (1973) and Graboske et al. (1973). The evolution of all the fifteen chemical species considered is explicitly followed without imposing them to be in equilibrium. Furthermore, the evolution of species having a number fraction greater than 10^{-8} is followed on a time scale corresponding to abundance variations smaller than 20%.

3.3. Optical atmosphere

The atmosphere is computed using the gray atmosphere approximation. We assume the temperature and optical depth are related by $T(\tau, T_{\rm eff})^4 = T_{\rm eff}^4\,[\tau + q(\tau)]3/4$. The Hopf function $q(\tau)$ is computed using an analytical relation obtained by solving the equation of radiative transfer adopting the Wick-Chandrasekhar method (see e.g. Collins II 1989). The diffusion approximation is used to compute the temperature gradient and the radiative pressure only when $\tau \approx 10$, since at this optical depth this approximation is guaranteed within 1% approximately. The stellar radius corresponds to an optical depth where $T(\tau_*) = T_{\rm eff}$.

3.4. Treatment of superadiabatic regions

The transport of energy in the convective envelopes is treated using the mixing-length theory (MLT) approximation (Vitense 1953; Böhm-Vitense 1958) or the Canuto and Mazzitelli (CM) model (Canuto & Mazzitelli 1991, 1992). Neither overshooting nor convective penetration (Zahn 1991) are considered in this work, since both effects are expected to be negligible in the mass range considered.

3.5. Opacities

For temperatures higher than 11 000 K we use the OPAL radiative opacity tables of Rogers & Iglesias (1994) computed taking the Grevesse & Noels (1993) relative metal abundances for the Sun. Whenever needed these opacities are completed with the opacities from the Los Alamos Opacity Library (LAOL, Huebner el al. 1977) computed with the Ross & Aller (1976) heavy elements mixture. For temperatures under 11 000 K we adopt the Neuforge (1993) opacity tables. If preferred it is possible to use the Kurucz (1992) opacity tables, which apply to hydrogen mass fractions close to 0.70. Both low-temperature sets were computed using the Anders & Grevesse (1989) mixture. The contribution of conductive opacity is also considered using the program of Hubbard & Lampe (1969).

3.6. Abundances

To compute the models we adopt an initial composition corresponding to the Grevesse & Noels (1993) mixture, except for the deuterium which is taken from Reeves (1994). The value adopted for [D/H], 1.65×10^{-5}, agrees with the one obtained by the Hubble Space Telescope for the stellar gas in front of Capella (Linsky et al. 1992) and with the values obtained along other lines of sight (Vidal-Madjar 1991; McCullough 1992). The mass fractions of hydrogen (X_o) and helium (Y_o) used in the initial composition of our models is always such that $Z_o/X_o = 0.0245$, where Z_o is the metallicity, in agreement with the most recent estimated value for the solar photosphere (Grevesse & Noels 1993).

4. Theoretical results

We computed evolutionary sequences of stars with masses 0.5, 0.7, 0.8, 0.9, 1.0, 1.1, 1.2, 1.3 and 1.5 $M_\odot$ from the top of the Hayashi track, corresponding to central temperatures of the order of 5×10^5 K, until the models reached the zero age main-sequence. The one solar mass models were further evolved up to the present age of 4.75×10^9 years, a value chosen according to the "Global Oscillations Network Group solar model comparison project" (Christensen-Dalsgaard 1991; Gabriel 1991). All the models were computed hydrodynamically (at constant mass) until central temperatures reached values of the order of 10^7 K, and hydrostatically afterwards.

For comparison we consider five sets of models each with different input physics concerning the high- and low-temperature opacities, the EOS and the treatment of superadiabatic convection. Summarising:

- M1: OPAL + LAOL high-temperature opacities, Neuforge low-temperature opacities, Coulomb corrections in the EOS and MLT convection treatment with the mixing distance given by $\lambda = \alpha H_p$, where H_p is the pressure scale height (for the determination of α, see further). This is our reference model.
- M2: same as M1 except that only LAOL opacities are used at high-temperatures.
- M3: same as M1 except that Kurucz opacities are used at low-temperatures.
- M4: same as M1 but excluding the Coulomb corrections in the EOS.
- M5: same as M1 but using the CM convection model with $\lambda = \alpha H_p$.

These choices are meant to represent the main uncertainties in the physics used to compute the stellar models. Models M2 and M3 explore the effect of uncertainties in the opacity coefficients: OPAL opacities are in general higher than the LAOL ones, specially around 30 000 K where the differences amounts to a factor 2 to 3 for the solar metallicity (Rogers & Iglesias 1992). On the other hand, Neuforge low-temperature opacities can differ from the Kurucz set by some 15% (Neuforge 1993). Model M5 explores the uncertainties in the treatment of superadiabatic convection by considering the energy flux transported by turbulent convection according to the CM model. In our study we choose to adopt the CM model with $\lambda = \alpha H_p$ rather than $\lambda = z$, where z refers to the distance to the top of the convective zone, because our 1.0 $M_\odot$ model computed using $\lambda = z$ fails to reproduce the effective temperature of the Sun by 6% (cf. Civelek & Kiziloğlu 1995), which is incompatible with the methodology used (see further). Anyway, working with $\lambda = \alpha H_p$, apart from being easier from the numerical point of view, is likely to give all the same an idea of what we could find with a convection model different from MLT.

All theoretical uncertainties referred to so far affect directly the temperature gradient throughout the star and are expected to influence the position of models in the Hertzsprung-Russell diagram (HRD), specially their effective temperatures along the Hayashi track. The model M4 is intended to account for the uncertainties in the EOS. The inclusion of Coulomb corrections can reduce the pressure and energy at the center of the Sun by as much as 5%. On the other hand, the correct evaluation of the continuum depression due to Coulomb interactions is crucial for an accurate computation of the partition functions, which in turn determine the ionisation state of the gas, specially for low-temperature configurations like PMS low-mass stars. Uncertainties in the EOS, mimicked by neglecting the effect of Coulomb interactions, are thus expected to lead to relatively important uncertainties in the theoretical results.

Therefore, by comparing the results obtained with each set of models we expect to be able to evaluate the variations due to different input physics and/or convection algorithms. This allows to discuss their importance with respect to the observational uncertainties.

For each of these models we started out fitting the solar radius and luminosity at 4.75×10^9 years with $Z/X = 0.0245$ in order to determine the values of the hydrogen and helium initial mass fractions, and the mixing parameter α. We adopted $R_\odot = 6.9599 \times 10^9 cm$ (Ulrich & Rhodes 1983) and $L_\odot = 3.86 \times 10^{33} ergs^{-1}$ (Bahcall & Ulrich 1988). The precision achieved in the fitting of $R_\odot$ and $L_\odot$ is better than 0.2 and 0.5 percent, respectively. Table 2 presents the results obtained for these parameters as well as for other physical quantities concerning the center of the Sun and the lower boundary of the convective envelope. The table also includes the corresponding results obtained by Charbonnel & Lebreton (1993, hereafter CL) and Morel et al. (1995) for comparison. Our models computed with the MLT lead to α values around 1.5, while the model computed with the CM model, M5, has α below unity. This agrees with the predictions of Canuto & Mazzitelli (1991). All these models have an initial helium abundance around 0.26, except the model computed without Coulomb corrections (M4) which has a higher Y_o value, 0.27. This result is due to the fact that Coulomb corrections decrease the pressure, specially in the central regions, and this has to be compensated by a decrease of the

Table 2. Parameters for the Sun using different models: hydrogen X_0 and helium Y_0 initial mass fractions, convection parameter α, metallicity Z, radius and temperature at the lower boundary of the convective envelope, central temperature, density and hydrogen mass fraction. CL93 stands for the Charbonnel & Lebreton (1993) solar model, while M95 stands for the Morel et al. (1995) solar model

	X_0	Y_0	Z	Z/X	α	r_{bcz} ($R_\odot$)	T_{bcz} (10^6 K)	T_c (10^6 K)	ρ_c (g cm^{-3})	X_c
M1	0.720	0.262	0.0176	0.0245	1.53	0.733	2.051	15.336	146.521	0.362
M2	0.723	0.259	0.0177	0.0245	1.50	0.744	1.930	15.358	144.777	0.371
M3	0.720	0.262	0.0176	0.0245	1.55	0.727	2.111	15.336	146.487	0.369
M4	0.710	0.273	0.0174	0.0245	1.45	0.735	2.030	15.460	150.520	0.355
M5	0.720	0.262	0.0176	0.0245	0.68	0.732	2.062	15.332	146.319	0.369
CL93	0.703	0.278	0.0190	0.0270	1.66	0.718	2.127	15.560	150.7	0.345
M95	0.714	0.269	0.0175	0.0245	1.77	0.733	2.033	15.38	148	0.364

mean molecular weight so that the solar luminosity is still maintained at solar age (e.g. CL). For this reason models including Coulomb corrections present lower central pressures, densities and temperatures, as well as a lower initial helium content with respect to the models computed without Coulomb corrections.

The results obtained with our reference model show some important differences with respect to the CL model, specially concerning the initial hydrogen and helium mass fractions. Since the CL model was computed using a set of opacity tables very similar to the one we used for M3, and taking into account that the results obtained with M1 and M3 are basically the same, we conclude that the differences found cannot be due to the different opacity sets used. As to the EOS, the CL model uses the so-called MHD EOS (Hummer & Mihalas 1988; Mihalas et al. 1988; Däppen et al. 1988) which is based on the "chemical picture" and includes Coulomb corrections using the Debye-Hückel model. Thus, the results obtained with this EOS for the Sun should not differ in a significant way from the ones of our EOS. Consequently the differences found should be mainly due to the higher Z value used by CL.

On the contrary, the results obtained with the Morel et al. (1995) model are very similar to ours. The opacities used are the same as in the CL model, while the EOS uses the Eggleton et al. (1973) formalism with the inclusion of Coulomb corrections. The atmosphere is computed using $T(\tau, g)$ laws derived from the atmosphere models calculated with the Kurucz (1991) ATLAS9 code. The differences found, specially concerning the value of the convection parameter α, should probably be due to the differences in the computation of the atmosphere.

In Fig. 1 we compare the HRD location of models M2 to M5 relatively to the reference model, including the corresponding isochrones. We see that models M1, M2 and M3 are not very different from each other (Figs. 1a and 1b). The M1 and M3 tracks and isochrones are almost coincident. This results from the fact that the Neuforge and Kurucz opacities differ at most by some 10-15% for the range of temperatures of interest. Model M3 leads to tracks slightly redder than M1. On the contrary, M4 and M5 show considerable differences when compared with the reference model (Figs. 1c and 1d). M4 leads to hotter tracks, while M5 produces tracks clearly shifted towards lower effective temperatures for ages in excess of approximately one million years.

Table 3. Theoretical mass and age ratios for the different models. Values correspond to the four possible locations of the binary in the HRD as listed in Table 1

	K4 - K4 (p - s)	K4 - K5 (p - s)	K5 - K4 (p - s)	K5 - K5 (p - s)	
M_p/M_s	1.01	1.28	0.81	0.99	M1
$\log t_p/t_s$	-0.27	0.04	-0.54	-0.25	
M_p/M_s	1.03	1.27	0.82	1.00	M2
$\log t_p/t_s$	-0.27	0.00	-0.54	-0.25	
M_p/M_s	1.03	1.30	0.81	0.99	M3
$\log t_p/t_s$	-0.26	0.04	-0.54	-0.25	
M_p/M_s	1.06	1.36	0.79	1.01	M4
$\log t_p/t_s$	-0.24	0.04	-0.52	-0.23	
M_p/M_s	1.02	1.21	0.82	0.95	M5
$\log t_p/t_s$	-0.28	-0.01	-0.55	-0.31	

5. Comparison with the observations

For each of these models we locate the binary in the HRD and determine the mass and age of each component by interpolation. We seek for models complying both with the dynamical mass ratio and the assumption of coeval formation of the binary components. In principle, coeval formation of binary components implies both components have the same age. However, there are uncertainties in the ages derived from the theoretical models, mainly due to the fact that the duration of the mass accretion phase is not taken into account in models evolving at constant mass (Mazzitelli 1989). The observed and theoretical mass accretion rates for the early phases of PMS evolution suggest the mass accretion phase can be relatively long (of the order of some million years) and different from star to star (e.g. Mazzitelli 1989; Palla 1993 and references therein). Hence, it is reasonable to assume coeval formation if the ages derived for each binary component differ by no more than 20%, i.e. if the value of $\log t_p/t_s$ lays approximately within 0.09. The results obtained are presented in Table 3. We see that all models are compatible with the assumption of coeval formation for a K4

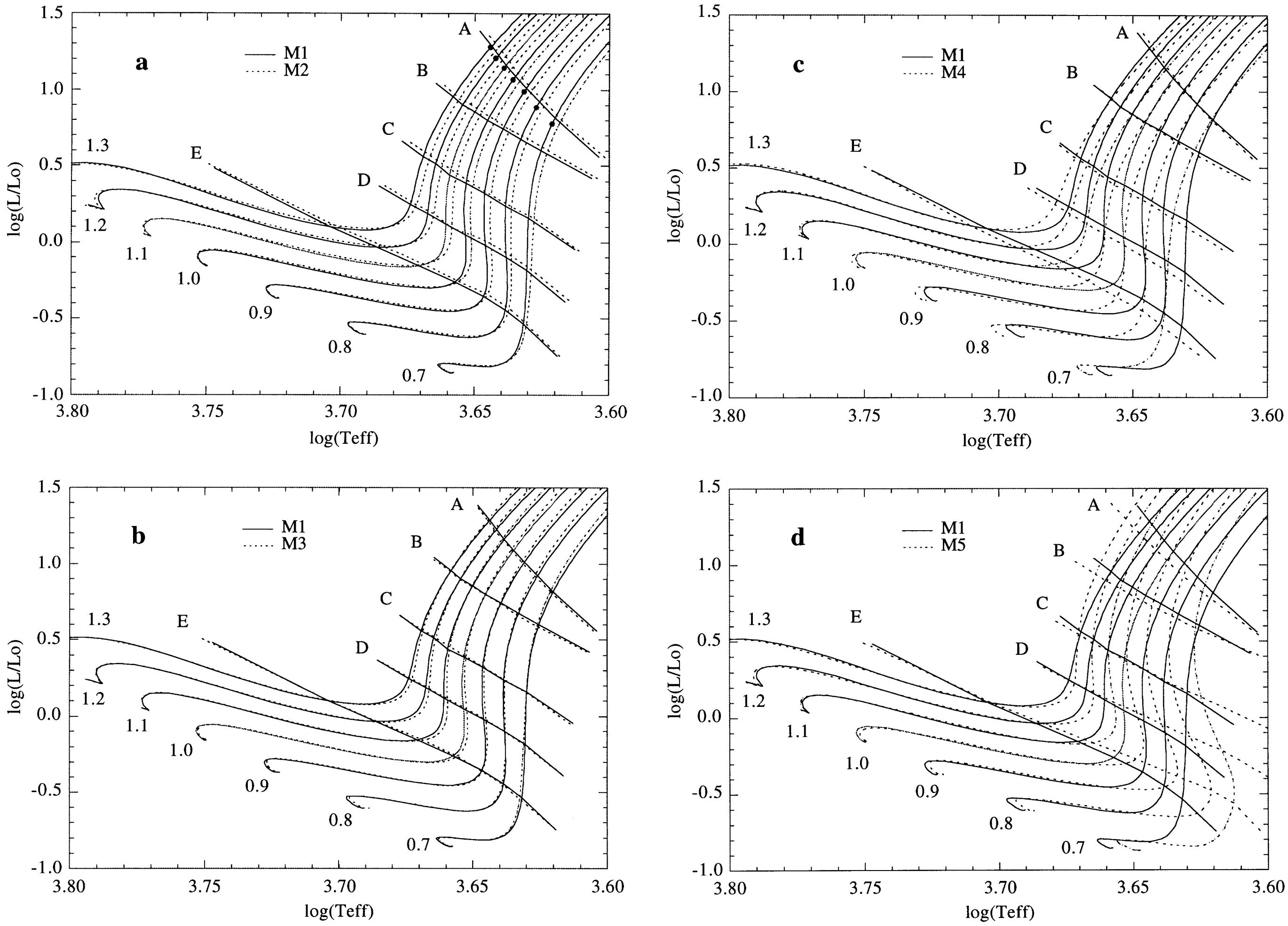

Fig. 1a–d. Comparison between HRD tracks and isochrones for different models: **a** M1-M2, **b** M1-M3, **c** M1-M4, **d** M1-M5. Isochrones shown correspond to 10^5 (A), 3×10^5 (B), 10^6 (C), 3×10^6 (D) and 10^7 (E) years. The circles in plot **a** correspond to the deuterium-main-sequence (Mazzitelli & Moretti 1980) for the reference model M1

primary and a K5 secondary, since the difference in age is always less than 20%. However, this spectral type combination fails to reproduce the dynamical mass ratio. All models lead to mass ratios higher than the dynamical one (1.09 ± 0.07). The M5 value is the one that stands closest to the dynamical value (1.21) while model M4 clearly leads to the worst result (1.36). On the other hand, the dynamical mass ratio is reproduced by all models for the K4-K4 and K5-K5 combination, but none of them agrees with the assumption of coeval formation of the components. The K5-K4 combination fails to reproduce the dynamical mass ratio and does not agree with the assumption of coeval formation.

Anyway these results were obtained using nominal effective temperatures and luminosities. They do not take into account the observational uncertainties. In fact, the conversion from spectral type to effective temperature depends on the scale used. However, the main contribution to the uncertainties in this quantity comes from the fact that this conversion is quantizised. It is well known that stars within a given spectral type can have different effective temperatures. There are also uncertainties in the luminosities specially due to uncertainties in the evaluation of the bolometric correction, extinction, distance and "veiling". Taking this into account and following the analysis of Lee (1992) and Hartigan et al. (1994) we may assume an uncertainty of $\Delta \log T_{\rm eff} = 0.01$ in $\log T_{\rm eff}$ and of $\Delta \log L/L_{\odot} = 0.07$ in $\log L/L_{\odot}$. These error bars define for each component an uncertainty domain in the HRD (see Fig. 2). In the following we shall consider that each domain is well represented by five $\log T_{\rm eff}$ - $\log L/L_{\odot}$ combinations, corresponding to the four vertexes of the box limiting the domain and its center. This choice allows twenty five possible combinations of primary-secondary locations in the HRD.

Therefore, we repeated the mass-age determinations for each of these combinations and compared the results obtained with the observational data. Only model combinations that fitted the dynamical lower mass limits were retained. For these combinations we checked again for agreement with the dynamical mass ratio interval, as well as the constraint of coeval formation. The results are presented in Fig. 3. Only the points inside the dashed box fulfil the two requirements mentioned above.

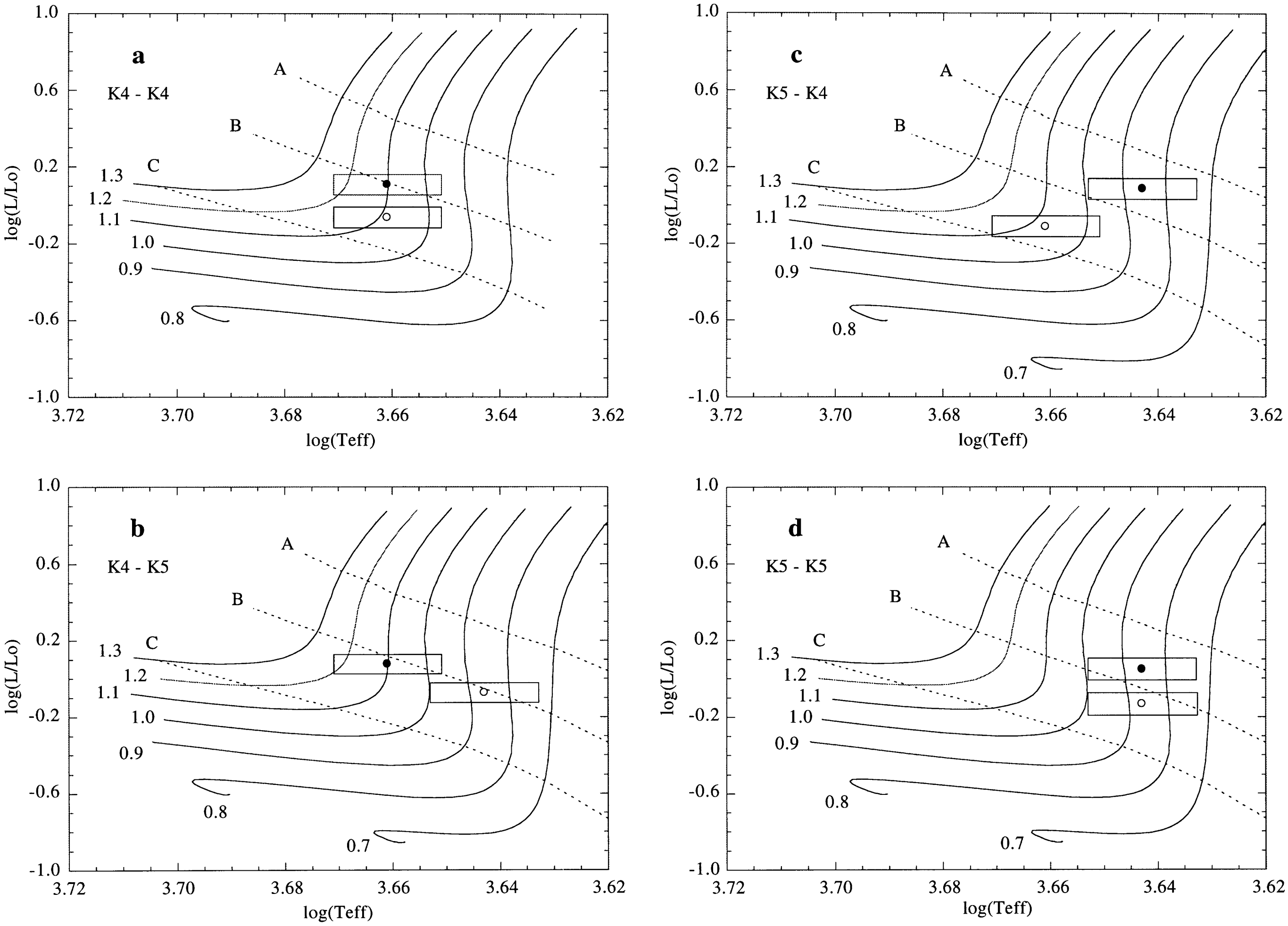

Fig. 2a–d. Uncertainty domains for different primary (filled circle) - secondary (open circle) spectral type combinations: **a** K4-K4, **b** K4-K5, **c** K5-K4, **d** K5-K5. Each box, centred on the nominal values of $\log T_{\rm eff}$ and $\log L/L_\odot$, is $2\ \Delta \log T_{\rm eff}$ wide and $2\ \Delta \log L/L_\odot$ high. Tracks and isochrones correspond to the reference model. Isochrones are presented for 10^6 (A), 3×10^6 (B) and 10^7 (C) years

As expected, the results for models differing only in the opacities (M1, M2 and M3) are rather similar, allowing only K4-K4 and K4-K5 combinations. The same happens with model M5 computed using the CM model with $\lambda = \alpha H_p$. All these models agree well with the observational constraints (Figs. 3a,b,c,e). On the contrary, we see that observations place severe constraints on the model computed without Coulomb corrections in the EOS (Fig. 3d). The relatively small number of points in Fig. 3d results from the fact that for this model a significant number of primary-secondary combinations violates the dynamical lower mass limits.

Lee (1992) made a similar analysis for the NTTS 162814-2427 binary using the theoretical tracks computed by VandenBerg with the MLT approximation and the theoretical tracks of Mazzitelli where the CM model is used with $\lambda = z$. For R_V = 5.0 he found good agreement between the Mazzitelli models and the observational data. On the contrary, he found the observations led to stringent constraints on the VandenBerg models.

For the K4-K5 combination models M1, M2 and M3 lead to primary and secondary masses close to 1.10 and 1.00 $M_\odot$, respectively, and an age of the order of 3.7 million years. For the same spectral type combination model M5 leads to slightly higher masses: 1.15 and 1.06 $M_\odot$ for the primary and secondary, respectively. This results from the fact that M5 tracks are cooler than the previous ones, yielding higher masses for a given effective temperature and luminosity (see Fig. 1d). The age derived using M5 rounds up to 4.0 million years, which is very similar to the values obtained with models M1, M2 and M3. Unfortunately, Lee does not give the mass and age values for which the observational data and the theoretical model he tested do agree. However, from his results and using only nominal values of the effective temperature and luminosity for the K4-K5 combination and R_V = 5.0 may suggest the following values: $M_{\rm p} \approx 1.15\ M_\odot$, $M_{\rm s} \approx 1.00\ M_\odot$ and an age around 3.1 million years for the VandenBerg models, or $M_{\rm p} \approx 1.31\ M_\odot$, $M_{\rm s} \approx 1.16\ M_\odot$ and an age of the order of 4.1 million years for the Mazzitelli models.

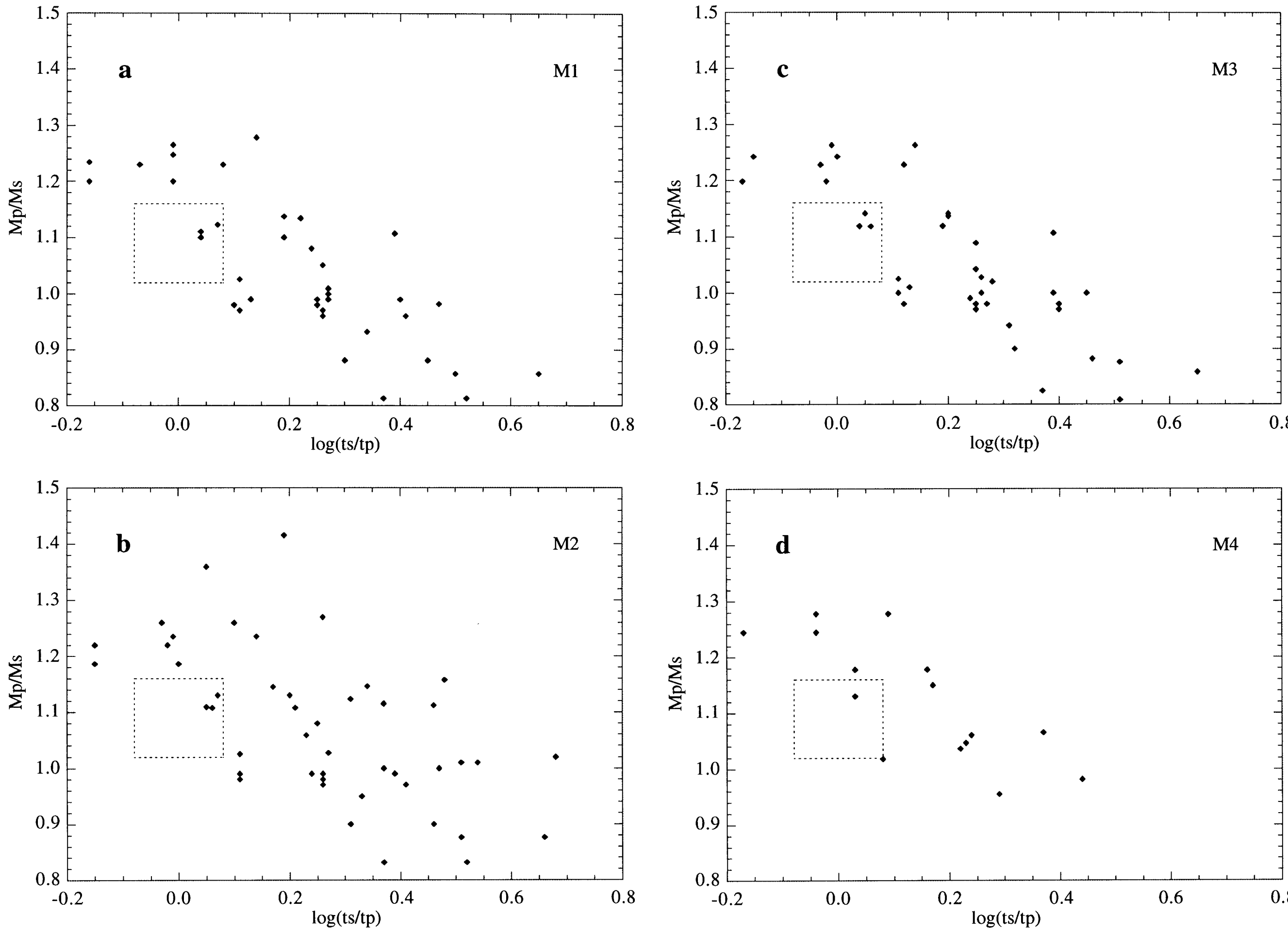

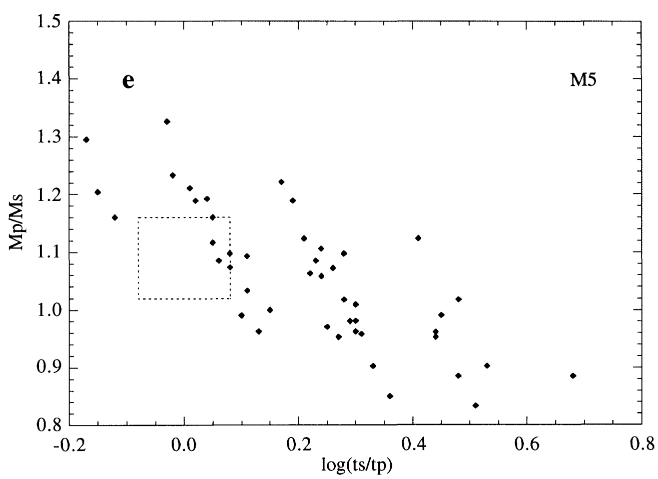

Fig. 3. Theoretical mass ratios versus age differences between the binary components for different primary-secondary locations in the HRD. Each plot corresponds to a different model: **a** M1, **b** M2, **c** M3, **d** M4, **e** M5. Points inside the dashed boxes correspond to primary-secondary combinations having mass ratios within the dynamical limits and ages compatible with the assumption of coeval formation of the binary components

The K4-K4 combination leads to a relatively wide range of masses and ages even within a given model. The primary and secondary masses range from 1.10 (M1) to 1.24 (M5) and 0.98 (M1) to 1.13 (M5) solar masses, respectively. The age ranges from 3 (M1) to 5 (M5) million years.

We can estimate the uncertainty in the mass and age determinations due to the observational uncertainties by looking at the spread in the masses and ages obtained for a given set. For M1, masses and ages can differ by up to a factor two and five, respectively. The results for the other sets are rather similar. This considerable mass spread is mainly due to the uncertainties in the effective temperature and the fact that the HRD tracks near the location of the binary are almost vertical. On the other hand, the age spread is caused not only by the uncertainties in the luminosity, but also by the uncertainties in the effective temperature since the isochrones are clearly not horizontal.

6. Conclusions

We have compared the most recent observational data available for the double-lined PMS binary NTTS 162814-2427 with theoretical models using different input physics for the opacities, the equation of state and the treatment of superadiabatic convection. All models, except the one computed without Coulomb corrections in the EOS, are in good agreement with the dynamical mass ratio and the assumption of coeval formation of the binary components. Thus, although the observational data are not able to provide tight constraints to the input physics used in the stellar evolution models, namely on the choice of the opacity sets and the treatment of superadiabatic convection used, they are nevertheless able to corroborate the importance of including the effects of Coulomb interactions between charged particles while computing the EOS.

Our results also show that the main contribution to the uncertainties in the mass and age determinations comes from the observational uncertainties, which are considerably higher than the theoretical ones. Therefore, more accurate determinations of effective temperatures and luminosities would be very useful to provide better mass and age estimates, and tighter constraints to the theoretical models.

Assuming a K4 primary and a K5 secondary, models differing only in the values of the opacity used lead to similar mass-age calibrations. In particular, our reference model yields: M_p = 1.10 $M_\odot$, M_s = 1.00 $M_\odot$ and an age of the order of 3.7 million years for the binary system. The values resulting from the CM convection treatment with $\lambda = \alpha H_p$ are only slightly higher: M_p = 1.15 $M_\odot$, M_s = 1.06 $M_\odot$, and an age of the order of 4.0 million years.

Acknowledgements. This research was co-financed by Centro de Matemática da Universidade do Minho, Centro de Astrofísica da Universidade do Porto and grant BD/346/90-RM from JNICT, Portugal. The author wishes to thank Prof. J.P. De Greve, Prof. M.T.V.T. Lago and Prof. C. de Loore for valuable suggestions to improve the manuscript. The author also wishes to thank the referee for the critical yet constructive comments.

References

Anders E., Grevesse N., 1989, Geochim. Cosmochim. Acta 53, 197
Bahcall J., Ulrich R.K., 1988, Rev. Mod. Physics 60, 296
Böhm-Vitense E. 1958, ZsAp 46, 108
Bouvier J., Appenzeller I., 1991, A&AS 92, 481
Broyles A.A., Sahlin H.L., Carley D.D., 1963, Phys. Rev. Lett. 10, 319
Canuto V.M., Mazzitelli I., 1991 ApJ 370, 295
Canuto V.M., Mazzitelli I., 1992 ApJ 389, 724
Cardelli J.A., 1988, ApJ 335, 177
Caughlan G.R., Fowler W.A., 1988, Atomic Data Nucl. Data Tables 40, 283
Charbonnel C., Lebreton Y., 1993, A&A 280, 666 (CL)
Christensen-Dalsgaard J., 1991. In: Gough D.O., Toomre J. (eds.) Challenges to Theories of the Structure of Moderate-Mass Stars. Springer Verlag, p. 11
Civelek R., Kiziloğlu N., 1995, A&A 297, 382
Clayton D.D., 1968, Principles of stellar evolution and nucleosynthesis. McGraw-Hill, New York, p. 381
Cohen M., Kuhi L., 1979, ApJS 41, 743
Collins II G.W., 1989, The Fundamentals of Stellar Astrophysics. W. H. Freeman and Company, New York, p. 263
Cox J.P., Giuli R.T., 1968, Principles of Stellar Structure. Gordon and Breach, Science Publishers, New York, p. 342
Däppen W., Mihalas D., Hummer D.G., Mihalas B.W., 1988, ApJ 332, 261
DeWitt H.E., Graboske H.C., Cooper M.S., 1973, ApJ 181, 439
Figueiredo J., 1996, in preparation
Eggleton P.P., Faulkner J., Flannery B.P., 1973, A&A 23, 235
Gabriel M., 1991. In: Gough D.O., Toomre J. (eds.) Challenges to Theories of the Structure of Moderate-Mass Stars. Springer Verlag, p. 51
Graboske H.C., Harwood D.J., Rogers F.J., 1969, Phys. Rev. A186, 210
Graboske H.C., DeWitt H.E., Grossman A.S., Cooper M.S., 1973, ApJ 181, 457
Grevesse N., Noels A., 1993. In: Prantzos N., Vangioni-Flam E., Cassé M. (eds.) Origin and Evolution of the Elements. Cambridge University, Cambridge, England, p. 14
Hartigan P., Strom K.M., Strom S.E., 1994, ApJ 427, 961
Hubbard W.B., Lampe M., 1969, ApJS 18, 297
Huebner W.F., Mertz A.L., Magee N.H., Argo, M.F., 1977, Astrophys. Opacity Library, UC-346
Hummer D.G., Mihalas D., 1988, ApJ 331, 794
Kurucz R.L., 1991. In: L. Crivellari, I. Hubeny, D.G. Hummer (eds.) Stellar Atmospheres: Beyond Classical Models, NATO ASI Series C, Vol. 341
Kurucz R.L., 1992, Rev. Mex. Astron. Astrofís. 23, 181
Landré V., Prantzos N., Aguer P., et al., 1990, A&A 240, 85
Lee C-W., 1992, Ph.D. thesis, Univ. Wisconsin, Madison
Linsky J.L., Brown A., Gayley K., et al., 1992, ApJ 402, 694
Mathieu R.D., 1994, ARA&A 32, 465
Mathieu R.D., Walter F.M., Myers P.C., 1989, AJ 98, 987 (MWM)
Mazzitelli I., 1989. In: Reipurth P. (eds.) Proc. ESO Conf. N. 33, Low Mass Star Formation and Pre-Main-Sequence Objects, p. 433
Mazzitelli I., Moretti M., 1980, ApJ 235, 955
McCullough P.R., 1992, ApJ 390, 213
Mihalas D., Hummer D.G., Däppen W., 1988, ApJ 331, 815
Montmerle T., Koch-Miramond L., Falgarone E., Grindlay J.E., 1983, ApJ 269, 182
Morel P., Provost J., Berthomieu G., Matias J., Zahn J.P., 1995. In: A. Noels, D. Fraipont-Caro, M. Gabriel, N. Grevesse, P. Demarque (eds.) Proc. of the 32nd Liège International Astrophysical Colloquium, Stellar Evolution: What Should Be Done, p. 395
Neuforge C., 1993, A&A 274, 818
Palla F., 1993. In: Mampaso A., Sanchez F. (eds.) Infrared Astronomy - IVth Winter School, Instituto Astrofísico de Canarias. Cambridge Univ. Press
Reeves H., 1994, Rev. Mod. Phys. 66, 193
Rogers F.J., Iglesias C.A., 1992, ApJS 79, 507
Rogers F.J., Iglesias C.A., 1994, anonymous ftp account
Ross J.E., Aller L.H., 1976, Sci 191, 1223
Shaviv G., Kovetz A., 1972, A&A 16, 72
Sauval A.J., Tatum J.B., 1984, ApJS 56, 193
Ulrich R.K., Rhodes E.J. Jr, 1983, ApJ 265, 551
Vidal-Madjar A., 1991, Adv. Space Res. Vol. 11, No. 11, p. 97
Vitense E., 1953, ZsAp 32, 135
Wilson R.E., 1981, A&A 99, 43
Zahn J.P., 1991, A&A 252, 179